



UNIVERSITY OF LEEDS

This is a repository copy of *Virtual prototyping of a semi-active transfemoral prosthetic leg*.

White Rose Research Online URL for this paper:

<http://eprints.whiterose.ac.uk/88701/>

Version: Accepted Version

Article:

Wei Lui, Z, Awad, MI, Abouhossein, A et al. (2 more authors) (2015) Virtual prototyping of a semi-active transfemoral prosthetic leg. Proceedings of the Institution of Mechanical Engineers, Part H: Journal of Engineering in Medicine, 229 (5). 350 - 361. ISSN 0954-4119

<https://doi.org/10.1177/0954411915581653>

Reuse

Unless indicated otherwise, fulltext items are protected by copyright with all rights reserved. The copyright exception in section 29 of the Copyright, Designs and Patents Act 1988 allows the making of a single copy solely for the purpose of non-commercial research or private study within the limits of fair dealing. The publisher or other rights-holder may allow further reproduction and re-use of this version - refer to the White Rose Research Online record for this item. Where records identify the publisher as the copyright holder, users can verify any specific terms of use on the publisher's website.

Takedown

If you consider content in White Rose Research Online to be in breach of UK law, please notify us by emailing eprints@whiterose.ac.uk including the URL of the record and the reason for the withdrawal request.



eprints@whiterose.ac.uk
<https://eprints.whiterose.ac.uk/>

Virtual prototyping of a semi-active transfemoral prosthetic leg

Zhen Wei Lui¹, Mohammed I Awad^{1,2}, Alireza Abouhossein¹, Abbas Dehghani¹ and Neil Messenger³

Abstract

This paper presents a virtual prototyping study of a semi-active lower limb prosthesis to improve the functionality of an amputee during prosthesis-environment interaction for level ground walking. Articulated ankle-foot prosthesis and a single axis semi-active prosthetic knee with active and passive operating modes were considered. Data for level ground walking was collected using a photogrammetric method in order to develop a base-line simulation model and with the hip kinematics input to verify the proposed design. The simulated results show that the semi-active lower limb prosthesis is able to move efficiently in passive mode, and the activation time of the knee actuator can be reduced by approximately 50%. Therefore, this semi-active system has the potential to reduce the energy consumption of the actuators required during level ground walking and requires less compensation from the amputee due to lower deviation of the vertical excursion of body centre of mass (BCOM).

Keywords

Virtual prototyping, dynamic modeling, transfemoral prosthesis, human gait

¹ School of Mechanical Engineering, University of Leeds, UK

² Mechanical Engineering, Ain Shams University, Egypt

³ School of Biomedical Sciences, University of Leeds, UK

Corresponding author:

Alireza Abouhossein, Institute of Design, Robotics and Optimisation (iDRO), School of Mechanical Engineering, University of Leeds, Leeds, LS2 9JT. Email: A.Abouhossein@leeds.ac.uk

Introduction

The loss of a limb has a devastating effect on any individual, especially if it is the lower limb as this is paramount to human locomotion. Every year, thousands of people around the world lose their lower limbs due to circulatory and vascular problems, complications of diabetes, cancer, or trauma. The effect of mobility loss reduces independence, affecting amputees' quality of life. It is difficult to obtain the exact number of lower limb amputees worldwide, as many countries do not keep a record of amputees or cause of amputations (1). However, some researchers (2, 3) have suggested that the total number of transfemoral amputees (TFA) worldwide is approximately seven million. Many of amputees are in need of lower limb prosthetic leg to return to their routine activities of daily living (ADLs). The total cost of a prosthetic leg is on average high. A lower extremity prosthetic leg may be priced ranging from \$5,000 to \$50,000 (4). Further, a report gathered by Williamson RB (5) to congressional members in United States government suggests that recent microprocessor-controlled knee can cost more than \$100,000. A large portion of the cost for prosthetic legs results from the recursive process used to improve mechatronics system design and testing. This may be reduced to a fraction of its original cost by using virtual prototyping to simulate the product for a variety of scenarios and sensitivity of the design factors. Virtual prototyping is a common technique used in the process of product development to validate the system design and its performance before implementing a physical prototype. This is done by creating a 3D virtual model which is then tested for different parameters and conditions. Colombo et al. used computer-aided design and virtual testing approach to validate the functionality of lower limb prostheses (6-8).

Recent advancement in materials, microcontrollers, sensors and actuators has had a direct effect on the prosthetic industries and has helped in the development of new state-of-the-art prosthetic devices. Consequently, the current transfemoral prostheses have been classified into three main groups as shown in Figure 1: *purely passive, active damping controlled and power controlled*. Purely passive prostheses, such as polycentric knee joint, four bar linkages, locking mechanisms and passive hydraulic cylinders, are mechanical mechanisms that require major controlling efforts from the amputee. Active damping

controlled prostheses were introduced during the 1990s with the release of the Intelligent Knee by Nabtesco, Intelligent Prosthesis (IP) by Blatchford, and C-Leg by Otto Bock. Above-knee amputees using active damping control prostheses must often compensate for both the knee and the ankle loss of function by regulating the energy input via the residual and the sound limbs. This is acceptable during most level ground walking phases and whilst descending stairs, as the net power required from the knee is negative and needs to be absorbed. However, these prostheses cannot provide the positive power required during other gait tasks, such as ascending stairs. Power controlled prostheses are fully actuated, for example the Victhom knee (9-11) which is commercially provided by Össur and known as Power Knee. These power controlled prostheses are actuated using either brushless DC motors (12-14), or by pneumatic actuators (15). Although powered prostheses are able to supply positive power, they consume more power than the human muscle, as they are continuously active.

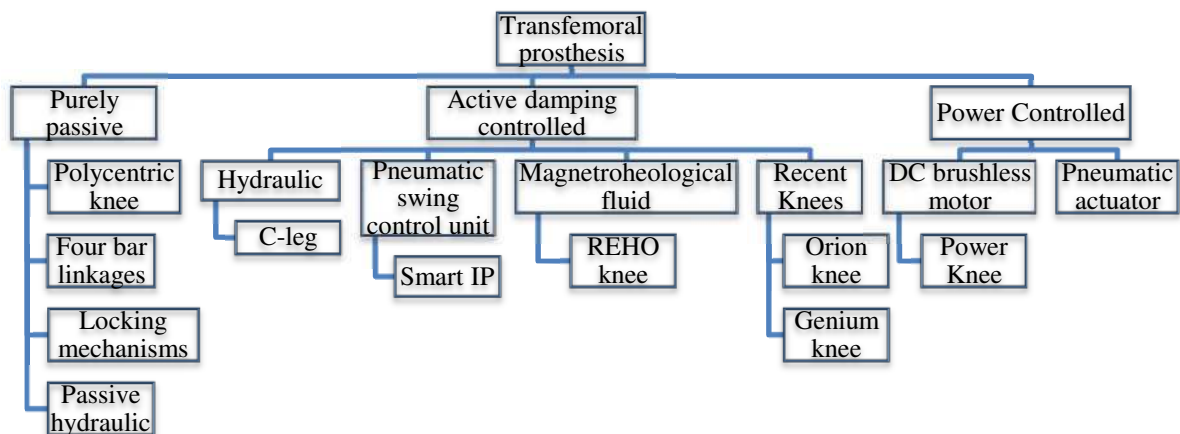


Figure 1: Classifications of the currently available lower limb prostheses.

Understanding the human walking mechanism is an important issue in designing efficient lower limb prostheses. The 'Ballistic walking' concept (16) was introduced in 1980 to explain natural walking. Ballistic walking is known as walking by vaulting over a relatively stiff straight stance leg (16, 17). This ballistic walking model helped to introduce the 'passive dynamic walking' concept (18, 19) in 1990. This

concept proved that completely passive dynamic walking machines powered only by gravity can walk in a way quite similar to humans, under modest inclines and with a little push. It provides an excellent natural gait on slopes without using actuators, relying solely on gravity and the inertia of the walking machine's segments. This concept explains how above-knee amputees with purely passive or active damping control prostheses can walk by controlling the hip movement. The energy is transferred from the residual limb (thigh) to the prosthetic knee, produces movement on the prosthetic knee due to *the dynamic coupling effect*. Therefore, the amputee's hip is considered the main engine and power source for voluntary control of the prosthesis. However, this requires more metabolic energy expenditure and mental effort in comparison to healthy subjects (20). Some researchers have provided passive dynamic bipedal walkers with just a little amount of energy added at the hip or ankle joints to walk on level ground (21-23). This type of walking utilizes *dynamic coupling interaction* between the segments by which more efficient ambulation with less energy expenditure is achieved. The main advantage of this novel approach in lower limb prosthetics is to use the *segment dynamics interactions* between amputee and the prosthetic leg to avoid stiff control associated with completely powered knees.

In general, amputees' energy expenditure has been used as an objective measure to gauge efficacy of a prosthetic leg. Amputees' energy expenditure has been suggested to be related to the six determinants components of gait, which are: pelvic rotation, pelvic tilt, knee flexion in stance phase, foot mechanism, knee mechanism, and lateral pelvic displacement (24). An increase in amputees' energy expenditure has been shown to increase vertical body center of mass (BCOM) (25, 26). Zelik et al. (2011) showed that spring stiffness used during the push-off phase in level ground walking in a prototype prosthetic foot will alter metabolic cost and BCOM in both amputated and intact subjects. Therefore, BCOM can be considered a concrete measure to represent the goodness of prosthetic leg design during ADLs (27-29).

Some daily life tasks require net positive power; such as ascending stairs, while others require net negative power at the knee joint; such as descending stairs. Therefore, there is a real need for developing a semi-active transfemoral prosthesis that can deliver the required positive energy when it is needed, and

work passively during other gait sub-phases. Although a hybrid hydraulic lower limb prosthetic system (30-32) based on semi-passive approach has been developed to adapt this concept, it has some issues associated with hydraulic actuation mechanisms such as; efficiency, response time, and number of components when compared to electrically actuated systems.

Therefore, the objective of this research was to design and test a proof of concept prosthetic knee and ankle for TFA based on an electrical actuator using a virtual prototyping approach which is capable of providing semi-active functionality similar to the human knee that is necessary to provide natural gait and to avoid the stiff control of a completely powered knee.

Materials and methods

A back-drivable, semi-active, prosthetic knee was designed to investigate the effect of dynamic coupling between the amputee's segments, the prosthetic leg and the ground. It was further explored how dynamic coupling from thigh to the knee may reduce power consumption of the knee actuator. This type of prosthesis is classified as a new generation of lower limb prostheses in which the negative and positive power across the joints are more naturally transferred and are comparable to the natural function of the human leg.

To reduce the product development cost, to evaluate and test the dynamic behaviour of amputee-prosthesis-environment interaction, and efficiency of semi-active prosthesis, a 3-dimensional (3D) dynamic virtual model of the proposed lower limb prosthesis has been developed using commercial software MSC.ADAMS® (Santa Ana, U.S.A). The computer model of the healthy subject consisted of 16 separate rigid bodies connected through series of revolute and fixed joints representing the complete bony structure of lower extremities and trunk, head, neck, and upper extremities. The physical properties for each segment was approximated by an ellipsoid based on anthropometric data by Zatsiorsky (33) for average human with height of 173 and 79 kg weight. The kinematic data of a lower limb in walking were collected using 3D motion capture and averaged to be imported to the computer model as input to the

model joints. A total of four able-bodied male subjects with a mean height of 172.5 cm (SD \pm 2.1 cm), body mass of 79.25kg (SD \pm 9.2kg), and age of 33 years (SD \pm 8.1years) volunteered to take part in this gait data collection study. All subjects signed the informed consent forms approved by the University of Leeds research Office of Good Practice & Ethics. All subjects were physically active and did not have any self-reported musculoskeletal disorders. Gait analysis experiments were carried out to obtain kinematic joint data during human level ground walking using a real time 3D motion capture system Qualisys ProReflex MCU240 and Track Manager (QTM) (Gothenburg, Sweden). The anatomical landmarks sites were palpated on individuals and the reflective surface markers were placed as illustrated in Figure 2. Each subject was required to walk at a self-selected walking speed along a straight path. The markers were labelled in QTM software and exported into C-Motion Visual3D V4 (Germantown, MD, U.S.A), which was used to define a rigid body model of pelvis, thigh, shank, and foot body segments for the lower limb. The joint angles versus time were exported from Visual 3D to MSC.ADAMS model and data were used to drive the joints using a cubic spline function.

Two force plates (AMTI, Force and motion, Watertown, MA. U.S.A.), placed in series, embedded into ground and synchronized with the motion cameras were used to determine critical gait events throughout gait cycle (e.g. heel strike and toe-off). ADAMS/Solver (C++) was used to solve the series of differential equations representing the physics of the human model with motion inputs at the driven joints.

To simulate a realistic contact between the foot and ground, the foot was designed with two separate rigid bodies for the metatarsal and the heel region. The initial ground contact point of the metatarsal was made shorter than that of the prosthetic foot length. This shorter ground contact point acted as a pivot point for the foot as the heel lifted off the ground. This point was then translated to the distal end of the metatarsal throughout terminal stance. The built-in contact algorithm in MSC.ADAMS was used to define contact between both anterior and posterior foot with the ground based on the penalty method in which the magnitude of the contact force is dominated by a fictitious penetration and stiffness parameter between two bodies. To create the boundary of a solid geometry ADAMS uses an automatic method to fit a solid

mesh to the defined geometry. Three-dimensional contact forces are calculated at each individual contact point and individual contributions are summed up to compute the net response of the system to the contact event. The built-in Coulomb friction was also included but only for anterior region of the foot contact with ground floor. The Coulomb friction was needed to prevent the anterior foot area from slippage.

The contact force (F_n) defined based on the following equation:

$$F_n = (K_c P)^n + C \frac{dP}{dt} \quad \text{Equation 1}$$

Where,

K_c : Contact stiffness

n : Contact exponent

C : Contact damping

P : Contact penetration

The contact parameters were set to $K_c=1.0+007$ N/m, $n=2.2$, damping= $1.0+005$ N/sec.m, penetration= 0.001 m in this simulation. Coulomb friction parameters were set to the following values: $\mu_{static}=0.7$, $\mu_{dynamic}=0.6$, stiction transitional velocity= 0.1 m/sec, Friction transition velocity: 1.0 m/sec.

These contact parameters were comparable to those values published by Pejhan et al.(34).

The healthy model was validated for domain of ground level walking at a self-selected speed (i.e. about 1.6 m/s) by comparing the displacement of vertical body center of mass (BCOM) with those obtained from experiments by Gard SA et al. (35) (Figure 3). The BCOM of the computer model in the vertical position was determined by adding the mass of every rigid body multiplied by its instantaneous location divided by the sum of all masses for each frame of integration in the simulation. A step was defined as the interval from initial contact of ipsilateral to the initial contact of the contralateral foot for purpose of comparison against the data presented by (35). The data was also normalized to remove any bias regarding the height of the participants in the experimental and the model. Figure 3 depicting the validation of the model.

[insert Figure 3.]

A unilateral TFA was simulated by a transversely cut of the right thigh in the healthy model about 40mm proximal above the knee. The attachment of the prosthesis to the stump leg was considered to resemble an osseointegrated transcutaneous press-fit distal femoral intramedullary device for above-the-knee prostheses (36, 37) with a hard point constraint (i.e. fixed joint). In the next section, the design of each part of the prosthetic leg is discussed.

Transfemoral prosthetic leg mechanical design

The details of the back-drivable semi-active knee design was explained by the authors in previous published work (38, 39). The essential elements of the design, shown in Figure 4, included: DC motor, transmission mechanism, bearings, ball screw and timing belt. This single-axis prosthetic knee had a maximum flexion angle of 105.1° . This range of operating angle was sufficient for normal walking as well allowing for sit to stand from a low chair with a maximum angle of 104.9° (40). The prosthetic knee model consisted of a motor with a power transmission unit connected to a ball screw. This screw and nut mechanism of the prosthetic knee was proposed to provide back-drivable motion and to allow the knee joint to move freely while it was not actuated. The total estimated weight of the prosthetic knee was 2.3kg. This prosthetic knee was fitted with a potentiometer sensor to sense the knee angle, and a load cell to measure the driving torque in active mode and the resistive torque in passive mode.

[insert Figure 4.]

The prosthetic knee in passive mode was designed in such a way that the energy transferred from residual segment to prosthetic leg due to the dynamic coupling assisted the movement of the under-actuated knee joint. In semi-active mode, the motor along with the dynamic coupling interaction drove the knee joint in an efficient manner by which net energy consumption is minimized.

The proposed prosthetic ankle-foot model had an articulated single-axis ankle that was postulated to have better versatility over a non-articulated prosthetic ankle in terms of manoeuvrability and adaptability. Figure 5 shows the CAD of the biologically inspired prosthetic ankle-foot model consisting of four main

parts (tibia, talus, calcaneus and metatarsal) and three spring-damper pairs (SD, SD1, SD2). These mechanical parts and spring pairs represented the bony and flexible structures of the human foot, respectively. The DC motor drives the screw and nut mechanism as shown in Figure 5a,5b altering SD1 (compression/extension) and enabled the prosthetic ankle-foot to have more adaptability as would be needed on different terrains. This actuation mechanism was modelled to mimic the muscle flexibility that exists in the gastrocnemius and soleus muscles, and to accommodate flexibility of the prosthetic ankle in the sagittal plane. The mechanical configuration, which is called a series elastic actuator (SEA) (41-44), provides high adaptability and interaction with the environment against different terrains, and allows energy to be stored during the loading response of stance phase and released during terminal stance. The advantage of this ankle mechanism design is particularly vivid during the stance phase. This SEA series design can easily mimic both the dorsiflexor and the plantarflexor muscles in a reciprocating fashion to prepare the foot for the start and end of the terminal stance. Apart from storing mechanical energy, the foot structure is postulated to be capable of absorbing shock during initial heel contact.

[insert Figure 5.]

Dynamic model and simulation of transfemoral amputee model

To reduce the product development cost, virtual prototyping techniques are used to validate system design and performance without the requirement to build a physical prototype. Simulation and software packages provide designers with the ability to iteratively develop and improve a model within the virtual environment. SolidWorks (Dassault Systèmes SolidWorks Corp., Vélizy-Villacoublay, France) was used to design the prosthetic knee and ankle. Three dimensional parts drawn in solid works were imported to the MSC.ADAMS® dynamic software (MSC software Corp., Santa Ana, U.S.A) and proper materials and coordinates were assigned to them for further evaluation. The prosthetic leg was integrated to the right leg using a fix joint as previously described and shown in Figure 6. The amputated model had 12 rigid bodies with corresponding mass and inertia as shown in Table 1. Three revolute joints were

accommodated at anatomical joints sites on the intact side connecting feet to shank, shank to thigh, and thigh to lower trunk providing flexibility needed in sagittal plane.

[insert Figure 6.]

Table 1: Mass and mass moment of inertia of the amputated human model

Segments	Mass (kg)	Ixx (kg·m ²)	Iyy (kg·m ²)	Izz (kg·m ²)
Head	5.067	3.11E-02	2.72E-02	1.61E-02
Neck	1.315	2.62E-02	2.62E-02	1.91E-02
Upper Torso	15.508	1.76E-01	1.39E-01	1.27E-01
Central Torso	7.541	5.30E-02	4.99E-02	3.29E-02
Lower Torso	8.708	7.74E-02	6.83E-02	3.91E-02
Left/Right Scapula	2.260	7.87E-03	7.87E-03	3.92E-03
Left/Right Upper Arm	2.007	1.41E-02	1.41E-02	1.96E-03
Left/Right Lower Arm	1.561	1.01E-02	1.01E-02	1.23E-3
Left/Right Hand	0.450	4.88E-04	4.88E-04	2.88E-04
Left Upper Leg	7.125	1.10E-01	1.10E-01	1.67E-02
Right Upper Leg	5.529	5.25E-02	5.23E-02	1.38E-02
Left Lower Leg	4.036	5.71E-02	5.71E-02	5.53E-03

On the amputated side (right) the thigh residual limb attached to lower trunk using a revolute joint in superior section, the inferior side was fixed to the prosthesis using a fixed joint. The virtual model was used to test the lower limb prosthesis performance when the knee and/or ankle were in one or more combinations of different control modes; passive, active or semi-active. In active mode, the prosthetic

knee joint was driven by the DC motor in such a way that the motion was similar to that of an intact knee joint. In the passive mode, the knee prosthesis was driven by the amputee's hip movement (i.e. dynamics coupling) and the ground reaction force.

[insert Figure 7.]

The active ankle provides floor clearance during swing phase and needed rigidity during stance phase. The combination of control modes were studied to observe the performance of the lower limb prosthesis at different operating conditions. The prosthetic knee deactivation mode occurred either at heel-off (HO) (D-Con1) or, in condition two (D-Con2), at toe-off (TO) (Figure 7). On the other hand, the activation for both former and latter conditions (A-Con1 and A-Con2) happened prior to heel strike (HS) to avoid premature initial contact of the un-actuated knee prosthesis.

[insert Figure 8.]

Human locomotion is a repetitive process, in which the walking phases and events are repeated in every gait cycle. Therefore, finite state control can be utilized to represent the control strategy of the prosthetic limbs. A finite state control (FSC), shown in Figure 8, was developed to simulate lower limb prosthesis during level ground walking when the prosthetic knee was semi-active, and prosthetic ankle-foot was active. A virtual force sensor was created to monitor the vertical ground reaction force (vGRF) on the calcaneus region. When designing a semi-active knee controller using finite state machine, there are two distinctive phases that should be carefully considered: swing and stance. During the stance control phase, the prosthetic ankle angle was measured, if there was no difference between the current and the initial value of the ankle angle and the force sensor at the calcaneus (the secondary transition condition) was off (HO), the prosthetic knee was deactivated. If the prosthetic foot was on the ground, the vGRF sensor was activated moving the ankle to the heel strike (HS). The activation was fulfilled, if the sensor monitoring the prosthetic knee angle satisfied the initial value of the knee angle at HS or the calcaneus strikes the

ground. The knee actuator was activated prior to HS to avoid any premature initial contact of the passive knee, which would cause gait disruption as well as an unsupported loading response.

Results

The motion capture results consist of the subjects' ankle and knee joint angles and the corresponding mean and standard deviation for several gait measurements as shown in Figure 9. The joint angles for lower extremity of both left and right side for 3 gait cycles were measured (Figure 8a, b, c). The plots were normalized over 4 seconds; this was the average time taken for an individual to complete 3 gait cycles.

[insert Figure9.]

Figure 10 shows the back-drivable characteristic of the above-knee prosthesis under different control scenarios, as well as the effects of different deactivation conditions as compared to the intact leg. The semi-active knee finite state control deactivated the actuator during mid-stance. The effects of different deactivation conditions on the knee dynamic response are shown in Figure 10 when the deactivation starts either with heel-off (D-Con1) or with toe-off (D-Con2) and the prosthetic ankle was passive.

[insert Figure 10.]

The most significant difference in the context of dynamic response between D-Con1 and D-Con2, as depicted in Figure 10, was that D-Con2 needed damping adjustment to the swing phase . The knee prosthesis was deactivated at about 35% (D-Con1) and activated at about 92% (A-Con2) of the gait cycle for heel-off (HO) deactivation condition. At toe-off (TO) deactivation condition (D-Con2), the knee prosthesis was deactivated at approximately 52% and resumed its actuation at about 95% (A-Con2) of the gait cycle. The total deactivation period was 57% and 43% of gait cycle for HO and TO (i.e. Con1) deactivation conditions, respectively. The result also indicates that the actuation time of the knee motor is reduced by approximately 50% of a gait cycle. This helped to reduce the overall energy consumption during the level ground walking.

[insert Figure 11.]

To observe the effects of active prosthetic ankle on the semi-active knee joint behaviour during swing and stance phases, the maximum nut position of SD1 was altered from 8 mm to 16 mm above its initial position. The change of nut position increased/decreased the internal force of SEA due to compression/tension in SD1.

The results in Figure 12 show that as the maximum nut position decreases, the knee extension deviation from reference value became less during swing phases. Moreover, the deviation of vertical excursion of body centre of mass (BCOM) of the human model also during terminal stance was reduced as shown in Figure 11. This indicates amputees energy expenditure can be reduced by an effective design.

[insert Figure 12.]

Figure 13 shows the reference ankle joint torque of an intact limb and the torques produced by SD1 about the prosthetic ankle joint for Configuration 1 and 2. As illustrated, the maximum torque produced by the passive configuration could not reach the desired joint torque of an intact limb. However, this maximum torque is increased gradually throughout mid-stance to an approximate value of 1.15Nm/kg with Configuration 2. From the simulation results, both of the prosthetic ankle controls managed to produce sufficient toe clearance to avoid the foot striking the ground during swing phase. Referring to the above argument, dorsiflexion of the ankle-foot prosthesis is not necessarily to produce toe clearance. However, it was included so as to generate a greater resistance force of SD1 to alleviate the slapping of the metatarsal during foot flat.

[insert Figure 13.]

Discussion

A semi-active back-drivable prosthetic leg (BDPL) capable of transferring energy in different gait control modes was implemented. The healthy model of human was validated for joint kinematics data and BCOM during level ground walking. The proposed prosthesis was integrated to the model as shown in Figure 6. The semi-active BDPL performance has been investigated under the level ground walking for a complete gait cycle in both passive and active modes using computer simulation. The active knee controller was driving the prosthetic knee during stance phase to a similar manner to that of the reference knee angle from a healthy subject. The passive operating mode in the semi-active knee deactivated the knee motor during terminal stance phase to allow the knee to flex freely before it swings. As the prosthetic knee deactivates, the joint rotates freely under the influence of gravity, momentum and dynamic coupling, causing flexion at the knee joint. The prosthetic knee provided the kinematic response in the passive mode quite similar to the reference knee. In the passive mode of the prosthetic ankle, the nut was fixed to its initial position resulting in the prosthetic foot being perpendicular to the tibia during swing phase. The spring-damper allowed the foot mechanism to store mechanical energy during initial stance phase helping to ease plantarflexion movement and release of energy during mid-stance. A proper plantarflexion and dorsiflexion for different terrains at the ankle joint can be achieved by controlling the nut position throughout the stance phase during the active mode.

The simulation results at different deactivation conditions of the prosthetic knee, when the ankle is passive, have shown that the semi-active back-drivable knee prosthesis has successfully used the effect of dynamic coupling caused by the hip flexion/extension during level ground walking. The knee prosthesis during level ground walking showed that the back-drivable mechanism is capable of performing un-actuated swing phase almost identical to a sound knee using the dynamic coupling behaviour. The result indicates that early deactivation lead to a potential reduction of electrical energy usage in the motor. This factor contributes potentially to battery life span that is critical in the power prosthesis. Amputees' energy expenditure is directly related to prosthetic leg design (45) which is shown to influence the amputee's

body center of mass (BCOM) displacement (25, 26). Under Con1, when the maximum nut position was set to the smallest value that the nut can travel, the vertical excursion of the body centre of mass (BCOM) is reduced, resulting in reduction of the total energy expenditure of amputees. When the maximum nut position of SD1 was set to the smallest, the internal force in the SEA was also reduced helping to ease dorsiflexion of the prosthetic foot during stance phase. The knee actuator early deactivation during terminal stance or initial swing phase helped to reduce the motor energy consumption.

The active finite state controller of the prosthetic ankle-foot successfully showed plantarflexion performance during terminal stance. In this controller, the actuation of the prosthetic ankle occurred during mid-stance and allowed the series of the elastic actuators (SEA) to store energy. The controller does not directly regulate the prosthetic ankle joint angle, but it provides mechanical adaptability and allows the ankle-foot to adapt to the walking surface during stance phase. This ability of the ankle-foot adaptation not only provides comfortable level ground walking, but also it potentially improves mobility in ascending and descending a ramp. It is planned that this will be addressed in future studies.

Although this semi active BDPL along with finite state machine controller model achieves robust forward progression and more natural walking of the human-prosthesis model during level ground walking, there are still several limitations with this modelling approach. One would be consideration of the damping at the peak of D-Con2 of the knee. Amputees have a tendency to adapt to the prosthesis(46) but in this simulation such ability is not included. Additional adaptation or compensatory movements on the sound limb of the amputee was not included, either.

The differences between a human joint with 6-degrees of freedom articulation surfaces and the ideal joints considered in the model must be stated. The kinematics differences between amputee and healthy participants are also acknowledged(47). The current virtual prototyping of the semi-active prosthesis using healthy participants as input motion to the hip is justified considering the amputees with longer stump length and those considered as active amputees (i.e. K3, K4 level). The level of amputation for TFA will change the muscles volume and geometry, influencing actuation and stabilization of the thigh

(48). The changes in kinematics of the hip joint on the prosthetic side have been shown to be directly proportional to stump length(49). The longer the residual limbs the less muscle atrophy and less kinematics deviation from healthy participants.

Many TFA wear a conventional socket that it is adjusted to conforms to the morphology of the residual limb. The stump position inside the socket changes throughout the day affecting amputees' gait adaptation level. However, relative repositioning and adaptation of the socket to the thigh were not considered. In this preliminary study, the attachment site of prosthetic leg to the stump leg resembles an osseointegrated transcutaneous prosthesis (36, 37) with hard point with no inter-segmental motion. In our future study, the relative translation of the socket with respect to the stump will be considered. The number of parameters influencing the outcome of a prosthetic leg design is quite large and individuals may choose different strategies to adapt to the prosthetic device. However, in this initial study some simplification by constraining the movement to the sagittal plane was considered to make the process of understanding the technique and its outcomes both manageable and viable. Changes in the biomechanical and control parameters of this low-fidelity model are explicitly helpful in predicting the prosthetic leg performance and understanding the effect of different parameters before process of physically manufacturing the prosthetic leg is implemented which is costly process. A High-fidelity model is going to be considered in future studies by including the movements in transverse and coronal planes.

Acknowledgement

This work is linked to the current research sponsored by EPSRC (EP/K020462/1).

References

1. The Rehabilitation of People with Amputations USA: United States Department of Defense, MossRehab Amputee Rehabilitation Program, MossRehab Hospital; 2004. Available from: <http://www.posna.org/news/amputations.pdf>.
2. Sup FC. A powered self-contained knee and ankle prosthesis for near normal gait in transfemoral amputees. United States -- Tennessee: Vanderbilt University; 2009.
3. Sup F, Varol HA, Mitchell J, Withrow TJ, Goldfarb M. Self-contained powered knee and ankle prosthesis: Initial evaluation on a transfemoral amputee. IEEE International Conference on Rehabilitation Robotics (ICORR); 23-26 June 2009. p. 638-44.
4. Turner R. Prosthetics Costs: Disabled World; 2009. Available from: <http://www.disabled-world.com/assistivedevices/prostheses/prosthetics-costs.php>.
5. VA Health Care: Spending for and Provision of Prosthetic Items: DIANE Publishing; 2011. Available from: <http://www.gao.gov/assets/320/310331.pdf>.
6. Colombo G, Facoetti G, Rizzi C. A digital patient for computer-aided prosthesis design. Interface Focus. 2013;3(2).
7. Colombo G, Facoetti G, Rizzi C. Virtual Testing Laboratory for Lower Limb Prosthesis. 2013.
8. Colombo G, Facoetti G, Regazzoni D, Rizzi C. A full virtual approach to design and test lower limb prosthesis. Virtual and Physical Prototyping. 2013;8(2):97-111.
9. Bedard S, inventorControl system and method for controlling an actuated prosthesis. United States 2004.
10. Bedard S, inventorControl device and system for controlling an actuated prosthesis. United States 2006.
11. Bédard S, Roy P-o, inventors; Victhom Human Bionics Inc. (Saint-Augustin-de-Desmaures, (Quebec), CA), assignee. Actuated leg prosthesis for above-knee amputees. United States 2008.
12. Fite K, Mitchell J, Sup F, Goldfarb M. Design and Control of an Electrically Powered Knee Prosthesis. IEEE 10th International Conference on Rehabilitation Robotics (ICORR); 13-15 June 2007; New York, USA, . p. 902-5.
13. Sup F, Varol HA, Mitchell J, Withrow T, Goldfarb M. Design and control of an active electrical knee and ankle prosthesis. 2nd IEEE RAS & EMBS International Conference on Biomedical Robotics and Biomechatronics (BioRob); 19-22 Oct. 2008; Scottsdale, AZ, 2008. p. 523-8.
14. Lawson B, Varol HA, Huff A, Erdemir E, Goldfarb M. Control of Stair Ascent and Descent With a Powered Transfemoral Prosthesis. IEEE Transactions on Neural Systems and Rehabilitation Engineering. 2013;21(3):466-73.

15. Sup FC, Goldfarb M. Design of a Pneumatically Actuated Transfemoral Prosthesis. ASME International Mechanical Engineering Congress and Exposition; November 5 – 10: ASME; 2006. p. 1419-28.
16. Mochon S, McMahon TA. Ballistic walking. *Journal of Biomechanics*. 1980;13(1):49-57.
17. Mochon S, McMahon TA. Ballistic walking: an improved model. *Mathematical Biosciences*. 1980;52(3-4):241-60.
18. McGeer T, editor Passive walking with knees. *Robotics and Automation, 1990 Proceedings, 1990 IEEE International Conference on*; 1990 13-18 May 1990.
19. McGeer T. Passive dynamic walking. *the international journal of robotics research*. 1990;9(2):62-82.
20. van den Bogert AJ, Samozov S, Davis BL, Smith WA. Modeling and Optimal Control of an Energy-Storing Prosthetic Knee. *Journal of Biomechanical Engineering*. 2012;134(5):051007-.
21. Wisse M. Essentials of dynamic walking; analysis and design of two-legged robots: Technical University of Delft; 2004.
22. Collins S, Ruina A, Tedrake R, Wisse M. Efficient bipedal robots based on passive-dynamic walkers. *Science*. 2005;307(5712):1082-5.
23. Collins SH, Ruina A, editors. A bipedal walking robot with efficient and human-like gait. 2005 IEEE International Conference on Robotics and Automation; 2005.
24. Saunders J, Inman V, Eberhart H. The major determinants in normal and pathological gait. *Journal of Bone & Joint Surgery*. 1953;35:543-58.
25. Zelik KE, Collins SH, Adamczyk PG, Segal AD, Klute GK, Morgenroth DC, et al. Systematic Variation of Prosthetic Foot Spring Affects Center-of-Mass Mechanics and Metabolic Cost During Walking. *Neural Systems and Rehabilitation Engineering, IEEE Transactions on*. 2011;19(4):411-9.
26. Gitter A, Czerniecki J, Weaver K. A reassessment of center-of-mass dynamics as a determinate of the metabolic inefficiency of above-knee amputee ambulation. *American journal of physical medicine & rehabilitation*. 1995;74(5):337-8.
27. Cavagna GA, Saibene FP, Margaria R. External work in walking. *Journal of Applied Physiology*. 1963;18(1):1-9.
28. Cavagna GA, Margaria R. Mechanics of Walking. *Journal of Applied Physiology*. 1966;21(1):271-8.
29. Kerrigan DC. A Tool to Assess Biomechanical Gait Efficiency: A Preliminary Clinical Study. *American Journal of Physical Medicine & Rehabilitation*. 1996;75(1):3-8.
30. Lambrecht BGA, Kazerooni H. Design of a semi-active knee prosthesis. *IEEE International Conference on Robotics and Automation (ICRA)*; 12-17 May 2009. p. 639-45.

31. Pillai MV, Kazerooni H, Hurwicz A. Design of a semi-active knee-ankle prosthesis. IEEE International Conference on Robotics and Automation (ICRA); 9-13 May2011. p. 5293-300.
32. Fairbanks DM, Zoss AB, Pillai MV, Schwartz M, Harding N, Rosa M, et al., inventors; Berkeley Bionics (Berkeley, CA, US),The Regents of the University of California (Oakland, CA, US), assignee. Semi-actuated transfemoral prosthetic knee. United States2010.
33. Zatsiorsky VM. Kinetics of human motion. Champaign, IL: Human Kinetics; 2002.
34. Pejhan S, Farahmand F, Parnianpour M, editors. Design optimization of an above-knee prosthesis based on the kinematics of gait. Engineering in Medicine and Biology Society, 2008 EMBS 2008 30th Annual International Conference of the IEEE; 2008: IEEE.
35. Gard SA, Miff SC, Kuo AD. Comparison of kinematic and kinetic methods for computing the vertical motion of the body center of mass during walking. Human Movement Science. 2004;22(6):597-610.
36. Aschoff HH, Kennon RE, Keggi JM, Rubin LE. Transcutaneous, distal femoral, intramedullary attachment for above-the-knee prostheses: an endo-exo device. The Journal of Bone & Joint Surgery. 2010;92(Supplement_2):180-6.
37. Branemark R, Berlin O, Hagberg K, Bergh P, Gunterberg B, Rydevik B. A novel osseointegrated percutaneous prosthetic system for the treatment of patients with transfemoral amputation: A PROSPECTIVE STUDY OF 51 PATIENTS. The Bone & Joint Journal. 2014;96B(1):106-13.
38. Awad M, Tee KS, Dehghani-Sanij AA, Moser D, Zahedi S. Analysis and Performance of A Semi-Active Prosthetic Knee. Proceedings of the International Conference on Mechanical Engineering and Mechatronics (ICMEM 2012); Ottawa, Ontario, Canada2012.
39. Awad M, Tee K, Dehghani A, Moser D, Zahedi S. Design of An Efficient Back-Drivable Semi-Active Above Knee Prosthesis. The 14th International Conference on Climbing and Walking Robots (CLAWAR2011); Sept. 6 – 8; Paris, France2011. p. 35-42.
40. Rowe PJ, Myles CM, Walker C, Nutton R. Knee joint kinematics in gait and other functional activities measured using flexible electrogoniometry: how much knee motion is sufficient for normal daily life? Gait and Posture. 2000;12:143-55.
41. Pratt GA, Williamson MM. Series elastic actuators. IEEE/RSJ International Conference on Intelligent Robots and Systems; August 5-9 1995; Pittsburgh, Pennsylvania, USA1995. p. 399-406.
42. Sensinger JW, Weir RFF. Design and analysis of a non-backdrivable series elastic actuator. IEEE 9th International Conference on Rehabilitation Robotics; June 28-July 1; Chicago, IL, USA2005. p. 390 - 3.
43. Walsh CJ, Paluska D, Pasch K, Grand W, Valiente A, Herr H. Development of a lightweight, underactuated exoskeleton for load-carrying augmentation. Proceedings of the 2006 IEEE International Conference on Robotics and Automation; May 2006; Orlando, Florida, USA2006. p. 3485 - 91.

44. Vallery H, Ekkelenkamp R, van der Kooij H, Buss M. Passive and accurate torque control of series elastic actuators. Proceedings of the 2007 IEEE/RSJ International Conference on Intelligent Robots and Systems; October 29 - November 2; San Diego, CA, USA2007. p. 3534 - 8.
45. Waters R, Perry J, Antonelli D, Hislop H. Energy cost of walking of amputees: the influence of level of amputation. *J Bone Joint Surg Am.* 1976;58(1):42-6.
46. Hak L, Houdijk H, Steenbrink F, Mert A, van der Wurff P, Beek PJ, et al. Stepping strategies for regulating gait adaptability and stability. *Journal of Biomechanics.* 2013;46(5):905-11.
47. Nolan L, Wit A, Dudziński K, Lees A, Lake M, Wychowański M. Adjustments in gait symmetry with walking speed in trans-femoral and trans-tibial amputees. *Gait & Posture.* 2003;17(2):142-51.
48. Jaegers SM, Arendzen JH, de Jongh HJ. Changes in hip muscles after above-knee amputation. *Clinical orthopaedics and related research.* 1995;319:276-84.
49. Jaegers SMHJ, Arendzen JH, de Jongh HJ. Prosthetic gait of unilateral transfemoral amputees: A kinematic study. *Archives of Physical Medicine and Rehabilitation.* 1995;76(8):736-43.

1
2
3
4
5
6
7
8
9
10
11
12
13
14
15
16
17
18
19
20
21
22
23
24
25
26
27
28
29
30
31
32
33
34
35
36
37
38
39
40
41
42
43
44
45
46
47
48
49
50
51
52
53
54
55
56
57
58
59
60

Figure 1: Classifications of the currently available lower limb prostheses.

Figure 2: Markers placement configuration on lower limb. (a) The exact anatomical site of the markers placement, (b) Markers placement in experimental setup.

Figure 3: Comparison of experimentally obtained and model predicted vertical displacement of body center of mass (BCOM). Shaded area indicates corridors based on experimental data (34).

Figure 4: Prosthetic knee CAD model. (a) Schematic diagram for the prosthetic knee, (b) Rear view, (c) side view, (d) front view, and (e) 3D CAD model.

Figure 5: Ankle-foot CAD model. (a) Prosthetic ankle-foot (side view), (b) Series Elastic Actuator (SEA) model.

Figure 6: Humanoid model in ADAMS/View environment.

Figure 7: Gait activation and deactivation for semi-active control of knee prosthesis.

Figure 8: Finite state control for level ground walking. (a) Prosthetic knee semi-active finite state control, (b) Prosthetic ankle active finite state control.

Figure 9: The collected motion data for the entire gait. (a) Right and left hip flexion/extension angle relative to pelvis, (b) Right and left knee flexion/extension angle relative to thigh, (c) Right and left ankle plantar-flexion/dorsiflexion angle relative to shank.

Figure 10: Prosthetic knee angle response during gait (— healthy subject's knee joint angle response, - - - heel-off deactivation condition, toe-off deactivation condition).

Figure 11: Prosthetic knee joint responses for D-Con1 with different maximum nut position of active prosthetic ankle control.

Figure 12: BCOM vertical displacement error of human model for knee D-Con1 with different maximum nut position during active prosthetic ankle control.

Figure 13: Ankle torque during two configurations D-Con2 and A-Con1(Knee passive, knee active-passive) compared against reference ankle torque of intact limb

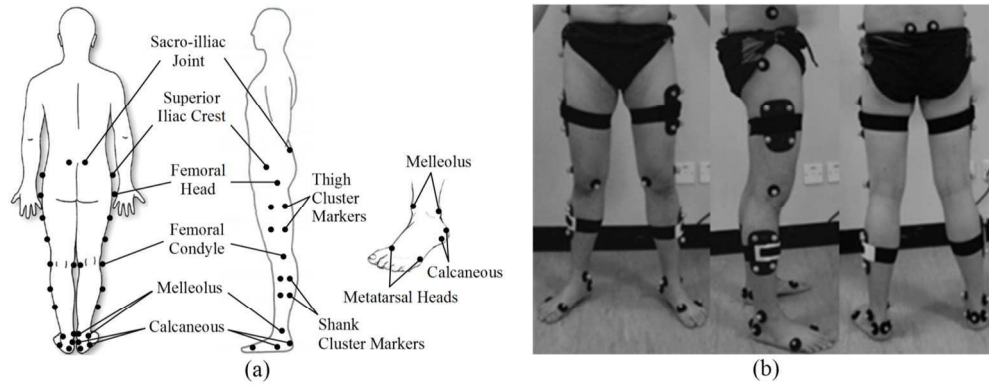


Figure 2: Markers placement configuration on lower limb. (a) The exact anatomical site of the markers placement, (b) Markers placement in experimental setup.

153x62mm (300 x 300 DPI)

1
2
3
4
5
6
7
8
9
10
11
12
13
14
15
16
17
18
19
20
21
22
23
24
25
26
27
28
29
30
31
32
33
34
35
36
37
38
39
40
41
42
43
44
45
46
47
48
49
50
51
52
53
54
55
56
57
58
59
60

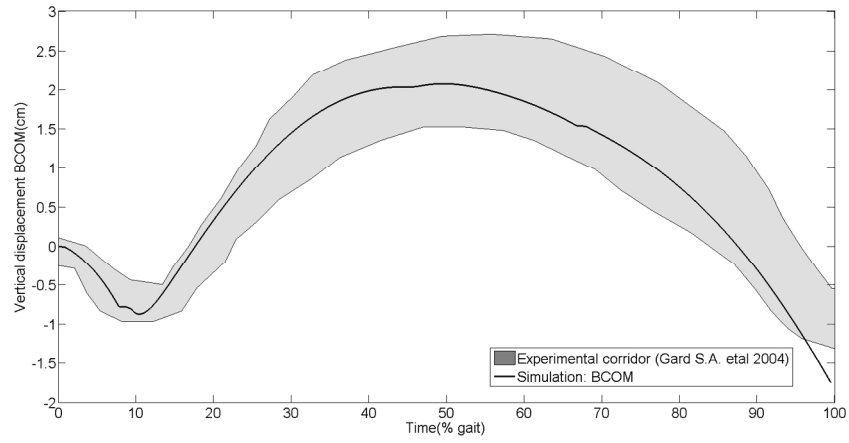


Figure 3: Comparison of experimentally obtained and model predicted vertical displacement of body center of mass (BCOM). Shaded area indicates corridors based on experimental data (34).
508x243mm (96 x 96 DPI)

Peer Review

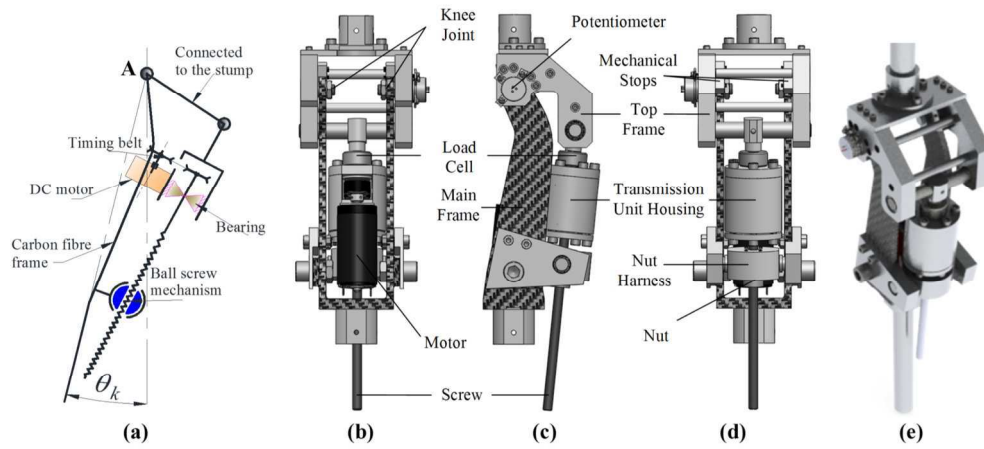


Figure 4: Prosthetic knee CAD model. (a) Schematic diagram for the prosthetic knee, (b) Rear view, (c) side view, (d) front view, and (e) 3D CAD model.
 160x75mm (300 x 300 DPI)

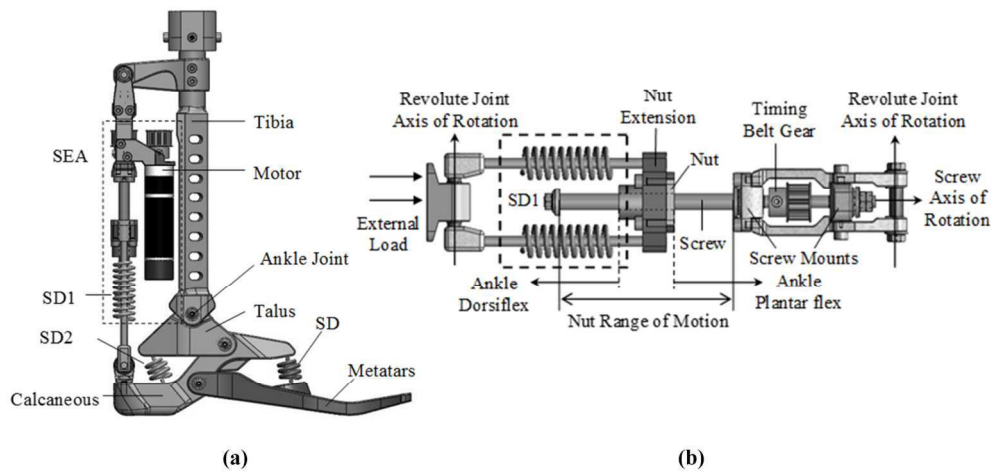


Figure 5: Ankle-foot CAD model. (a) Prosthetic ankle-foot (side view), (b) Series Elastic Actuator (SEA) model.

257x124mm (300 x 300 DPI)

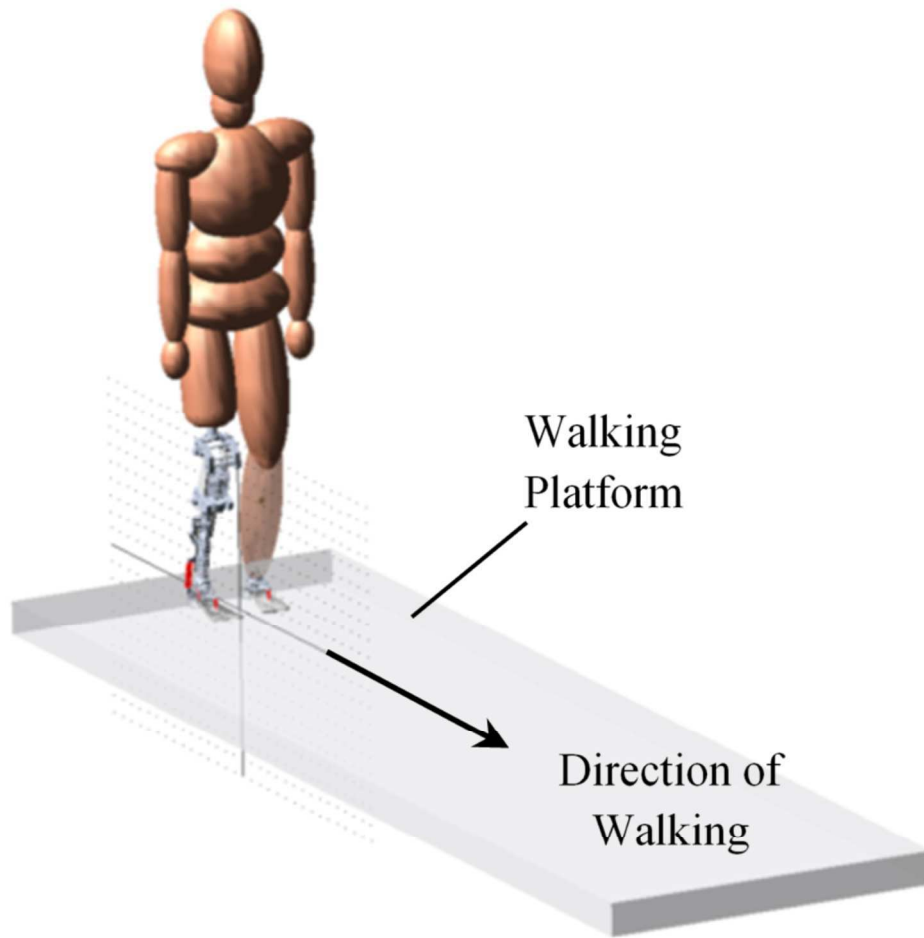


Figure 6: Humanoid model in ADAMS/View environment.
144x137mm (300 x 300 DPI)



1
2
3
4
5
6
7
8
9
10
11
12
13
14
15
16
17
18
19
20
21
22
23
24
25
26
27
28
29
30
31
32
33
34
35
36
37
38
39
40
41
42
43
44
45
46
47
48
49
50
51
52
53
54
55
56
57
58
59
60

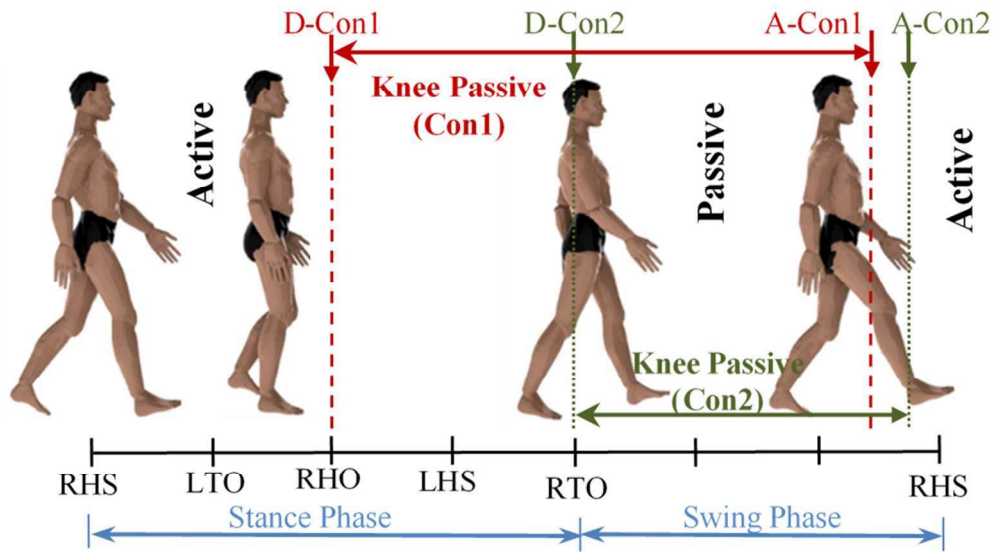


Figure 7: Gait activation and deactivation for semi-active control of knee prosthesis.
84x48mm (300 x 300 DPI)

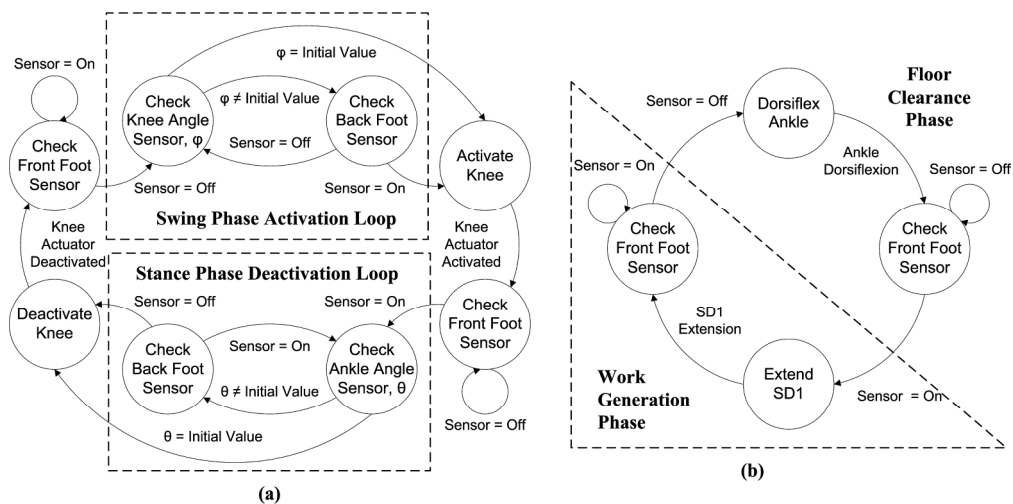


Figure 8: Finite state control for level ground walking. (a) Prosthetic knee semi-active finite state control, (b) Prosthetic ankle active finite state control. 108x53mm (600 x 600 DPI)

Peer Review

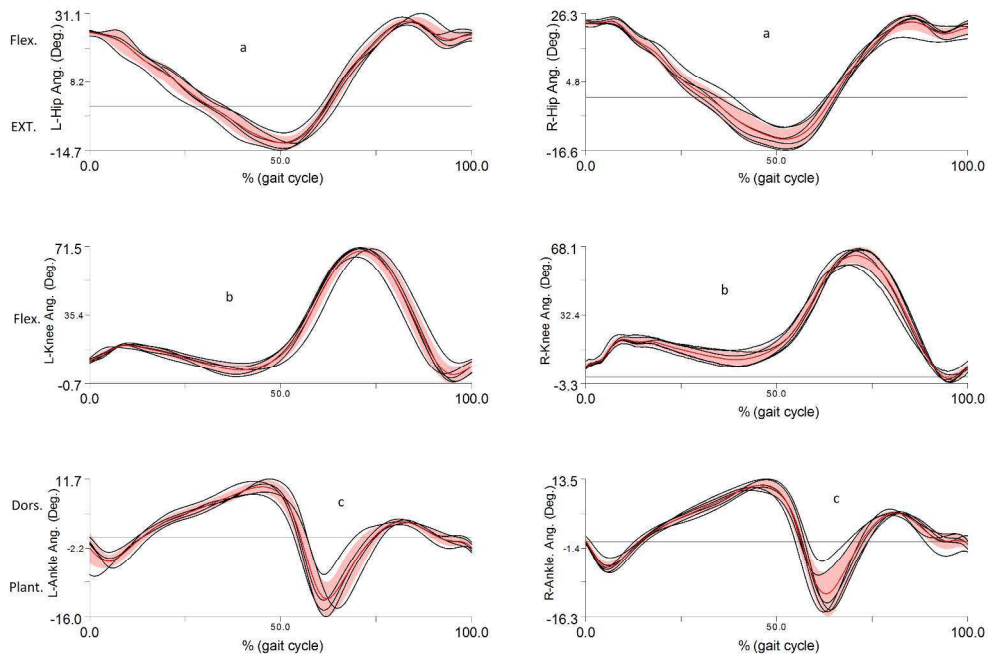


Figure 9: The collected motion data for the entire gait. (a) Right and left hip flexion/extension angle relative to pelvis, (b) Right and left knee flexion/extension angle relative to thigh, (c) Right and left ankle plantar-flexion/dorsiflexion angle relative to shank.
287x194mm (300 x 300 DPI)

Review

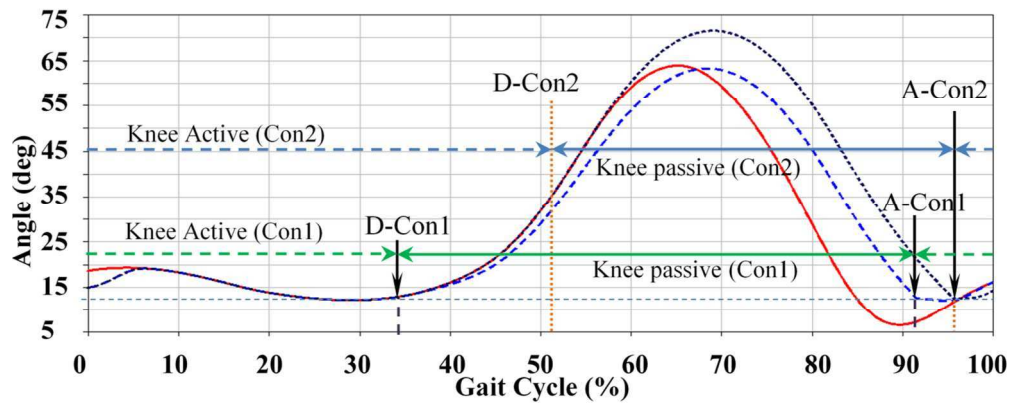


Figure 10: Prosthetic knee angle response during gait (healthy subject's knee joint angle response, heel-off deactivation condition, toe-off deactivation condition).
129x54mm (300 x 300 DPI)

1
2
3
4
5
6
7
8
9
10
11
12
13
14
15
16
17
18
19
20
21
22
23
24
25
26
27
28
29
30
31
32
33
34
35
36
37
38
39
40
41
42
43
44
45
46
47
48
49
50
51
52
53
54
55
56
57
58
59
60

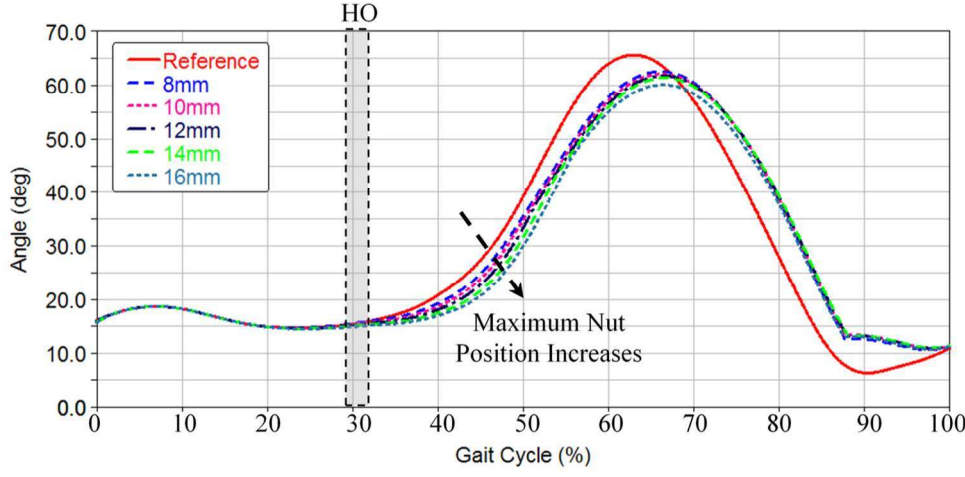


Figure 11: Prosthetic knee joint responses for D-Con1 with different maximum nut position of active prosthetic ankle control. 136x65mm (300 x 300 DPI)

Peer Review

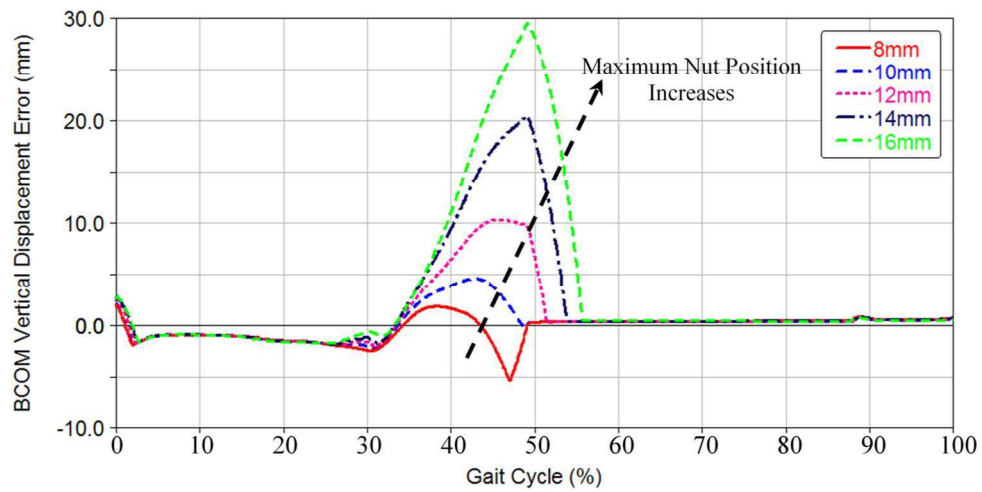


Figure 12: BCOM vertical displacement error of human model for knee D-Con1 with different maximum nut position during active prosthetic ankle control.
136x71mm (300 x 300 DPI)

1
2
3
4
5
6
7
8
9
10
11
12
13
14
15
16
17
18
19
20
21
22
23
24
25
26
27
28
29
30
31
32
33
34
35
36
37
38
39
40
41
42
43
44
45
46
47
48
49
50
51
52
53
54
55
56
57
58
59
60

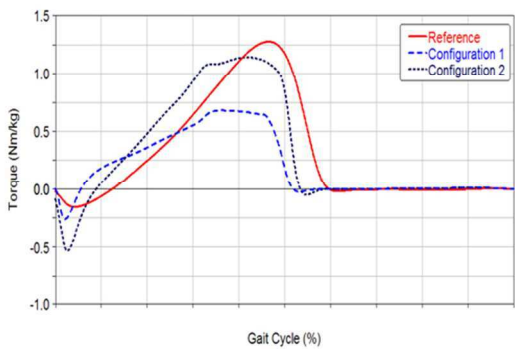


Figure 13: Ankle torque during two configurations D-Con2 and A-Con1(Knee passive, knee active-passive) compared against reference ankle torque of intact limb
254x190mm (96 x 96 DPI)

Review